# Grain-boundary effects on the magnetoresistance properties of perovskite manganite films

A. Gupta
*IBM Research Division, T. J. Watson Research Center, Yorktown Heights, New York 10598*

G. Q. Gong
*Department of Physics, Brown University, Providence, Rhode Island 02912*

Gang Xiao
*IBM Research Division, T. J. Watson Research Center, Yorktown Heights, New York 10598 and Department of Physics, Brown University, Providence, Rhode Island 02912*

P. R. Duncombe, P. Lecoeur, and P. Trouilloud
*IBM Research Division, T. J. Watson Research Center, Yorktown Heights, New York 10598*

Y. Y. Wang and V. P. Dravid
*Materials Science and Engineering Department, Northwestern University, Evanston, Illinois 60208*

J. Z. Sun
*IBM Research Division, T. J. Watson Research Center, Yorktown Heights, New York 10598*
(Received 7 October 1996)

The role of grain boundaries in the magnetoresistance (MR) properties of the manganites has been investigated by comparing the properties of epitaxial and polycrystalline films of $La_{0.67}D_{0.33}MnO_{3-\delta}$ ($D$=Ca, Sr, or vacancies). While the MR in the epitaxial films is strongly peaked near the ferromagnetic transition temperature and is very small at low temperatures, the polycrystalline films show large MR over a wide temperature range down to 5 K. The results are explained in terms of switching of magnetic domains in the grains and disorder-induced canting of Mn spins in the grain-boundary region. [S0163-1829(96)51746-7]

The recent observation of anomalously high magnetoresistance (MR) in the $La_{1-x}D_xMnO_{3-\delta}$ ($D$=Ba, Sr, Ca, Pb, or vacancies) system has spurred renewed interest in studying these doped perovskites.[1,2] Besides fundamental understanding, the studies have also been motivated by the potential field-sensor and device applications of these materials. A number of structural and magnetotransport studies of polycrystalline, single-crystal, and thin films of the doped manganites have appeared in the literature over the past year.[3–12] While there is a consensus emerging regarding a number of characteristic features of the MR behavior, the role of grain boundaries in the magnetotransport properties remains poorly understood and has been a major source of discrepancy in the literature.[6] With better understanding it may be possible to exploit the grain-boundary properties for practical applications, as in the case of the high-$T_c$ superconducting quantum interference devices (SQUID's).[13]

Significant differences in the MR of polycrystalline and single-crystal samples have been reported. In particular, bulk polycrystalline samples have shown substantial MR at temperatures much below the ferromagnetic transition temperature ($T_c$),[4–8] while the MR magnitude is usually very small in single crystals or epitaxial films of the same composition.[6,9–12] To clarify the role of grain boundaries in the MR behavior of manganites we have directly compared the properties of epitaxial and polycrystalline films of $La_{0.67}Ca_{0.33}MnO_3$ (LCMO), $La_{0.67}Sr_{0.33}MnO_3$ (LSMO), and $La_{0.75}MnO_3$ (LXMO) films,[10] each with a different $T_c$, grown on single-crystal and polycrystalline $SrTiO_3$ substrates. We find that, unlike the epitaxial films, the polycrystalline films indeed show substantial MR over a wide temperature range in all three systems. Our results indicate that domain boundaries are strong spin-dependent scattering centers. Magnetic Kerr microscopy has revealed that the magnetic domains in the polycrystalline samples are defined by the grains and they mostly switch independently in a field. The MR due to switching of magnetic domains has been determined to be ~20% and occurs at relatively low fields (<2000 Oe). Using grain boundaries to manipulate magnetic behavior may thus prove to be a useful method for significantly improving the low-field sensitivity of these materials.

The experimental system used for growth of manganite films using pulsed laser deposition has been described previously.[10] Thin films, with thickness of about 1000 Å, were grown on (100)-oriented single-crystal and polycrystalline $SrTiO_3$ substrates using appropriate targets. The polycrystalline $SrTiO_3$ substrates were obtained by cutting and polishing sintered pellets (97–98% density) of the material. To prepare the pellets, high-purity $SrTiO_3$ powder (average particle size <2 $\mu$m) was isostatically pressed and sintered between 1575–1675 °C. The time and temperature of sintering were varied to obtain samples with average grain size of 24, 14, and 3 $\mu$m. The films were characterized using x-ray diffraction and transmission electron microscopy (TEM). The cation stoichiometry of the films determined from Rutherford backscattering spectroscopy analyses, and independently confirmed by quantitative x-ray microanalysis in TEM, were within 5% of the nominal target compositions. Resistivity of the films was measured using a standard four-probe dc method. Magnetic measurements were carried out

 

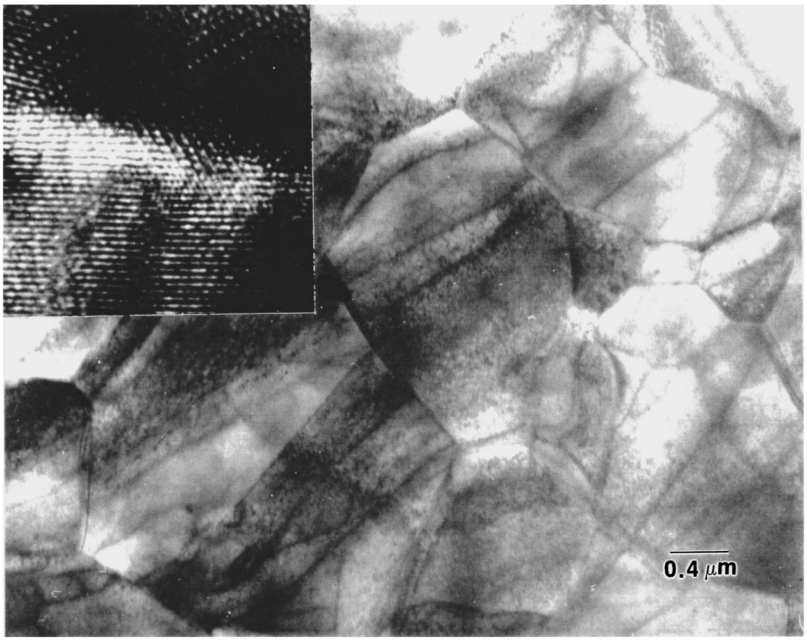


FIG. 1. Plan-view TEM image of a LCMO film grown on 3 $\mu$m average grain-size polycrystalline $SrTiO_3$ substrate. A well-defined grain morphology reminiscent of the underlying grain structure of the substrate is visible. High-resolution TEM image of a grain-boundary region is shown in the inset.

with a SQUID magnetometer. In both measurements the magnetic field was applied parallel to the plane of the substrate. A wide-field Kerr microscope was used for magnetic imaging of the domain structure at room temperature.[14]

Figure 1 shows an overall plan view of a LCMO film grown on a polycrystalline-$SrTiO_3$ substrate. The polycrystalline nature of the underlying substrate with an average grain size of about 3 $\mu$m is well replicated by the LCMO film. Although the film is grown on polycrystalline $SrTiO_3$, cross-sectional TEM images clearly showed the local epitaxial growth on individual $SrTiO_3$ grains. The high-resolution image of the grain-boundary (GB) region, shown as an inset in Fig. 1, reveals that the GB's in the film are well structured with local disorder as expected for polycrystalline GB's. Independent TEM and x-ray diffraction measurements of a LCMO film grown on a single-crystal (100) $SrTiO_3$ substrate have confirmed epitaxial growth of the film, with a pseudocubic structure.

The temperature ($T$) dependences of the resistivity ($\rho$) at different magnetic fields ($H$) are shown in Fig. 2 for an epitaxial film and polycrystalline LCMO films with three different grain sizes. The peak resistivity ($\rho_{\max}$) occurs at about the same $T$ ($\sim$230 K) for all the samples. This is very close to the $T_c$ determined from magnetization measurements. It is interesting to note that while the drop in $\rho$ at lower temperatures is quite sharp for the epitaxial film, the decrease occurs more slowly for the polycrystalline films. Moreover, the zero-field $\rho$ increases systematically with decreasing grain size over the whole range of $T$. This is not surprising considering that $\rho$ is increasingly influenced by the presence of GB's which act as regions of enhanced scattering for the conduction electrons. If the polycrystalline films are idealized to consist of low-resistivity ($\rho_1$) grains of size $L$ separated by thin GB layers of width $L'$ and high-resistivity $\rho_2$, then the effective resistivity is given by $\rho \cong \rho_1 + (L'/L)\rho_2$.[15] Indeed, an almost linear increase in the residual $\rho$ at 10 K is noted as a function of the reciprocal grain size for the LCMO (and also LXMO) films, as shown in the inset of Fig. 2. From the slope the specific GB resistivity ($L'\rho_2$) is estimated to be $\sim 6\times 10^{-5}$ $\Omega$ cm$^2$, with contributions from both magnetic and structural disorder scattering as will be discussed later.

The $T$ dependences of the MR ratio as a function of $H$ (0.5–4 T) for the 3 $\mu$m polycrystalline and the epitaxial film are plotted in Fig. 3. The MR ratios for the different fields are defined according to $\Delta\rho/\rho_H = (\rho_0 - \rho_H)/\rho_H$, where $\rho_0$ is the zero-field resistivity and $\rho_H$ is the resistivity in the applied field, $H$. For the epitaxial film, the MR ratio has a sharp peak at a $T$ slightly below $\rho_{\max}$ and is very small at low temperatures. Furthermore, it is observed that with increasing $H$ the MR ratio increases and the peak moves closer to the $T$ for $\rho_{\max}$ in zero field. The polycrystalline film exhibits a similar behavior. However, in addition, there exists a significant MR below $\rho_{\max}$ which is essentially independent of

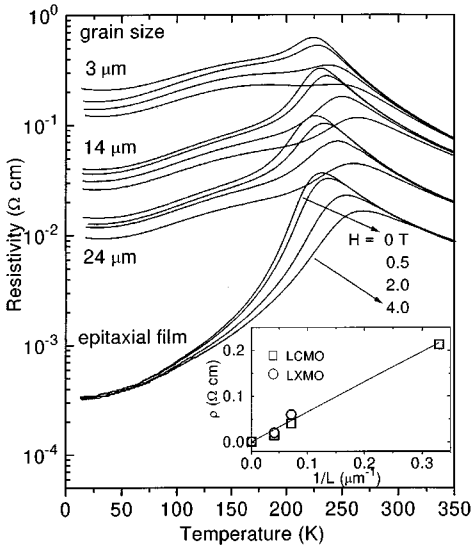


FIG. 2. Resistivity (in log scale) as a function of temperature for polycrystalline (average grain size of 3, 14, and 24 $\mu$m) and epitaxial LCMO films. For each sample, data measured at magnetic fields of 0, 0.5, 2, and 4 T are presented. The inset shows a plot of the zero-field resistivity at 10 K as a function of the inverse grain size ($1/L$) for LCMO and LXMO films.

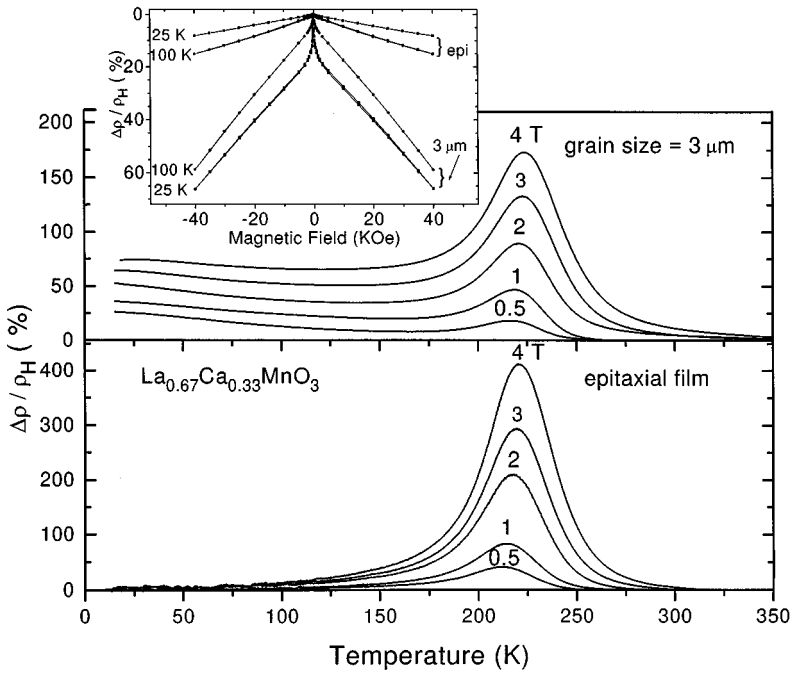


FIG. 3. Magnetoresistance (MR) ratio as a function of temperature for polycrystalline (3 $\mu$m average grain size) and epitaxial films of LCMO. Data for $H=0.5$, 1, 2, 3, and 4 T are presented for each sample. The inset shows the dependence of the MR ratio as a function of $H$ for the two films measured at 100 and 25 K.

$T$. The $H$ dependence of the MR ratio at 100 K and 25 K is plotted as an inset in Fig. 3. The MR ratio for the epitaxial film is small at both temperatures, increasing almost linearly with $H$ (7–15% at 4 T). A significantly larger drop (60–65 % at 4 T) over the same field range occurs for the polycrystalline film. In fact, the decrease is actually somewhat higher at 25 K than at 100 K. At 25 K, a sharp drop is observed at low $H$ ($<$2000 Oe) followed by a more gradual drop at higher values. The low-field drop is correlated with switching of magnetic domains as will be discussed later. We have observed a very similar $H$ dependence of the $\rho$ and the MR ratio for epitaxial and polycrystalline films of LXMO and LSMO with $T_c$ values of 250 K and 350 K, respectively.

The magnetotransport behavior near $T_c$ in the manganites has been attributed to a strong coupling between the conduction electrons and the local magnetic moment through the so-called double-exchange mechanism.[16] With decreasing $T$, the $\rho$ drops rapidly as the neighboring spins become aligned and the magnetization approaches its saturation value. One would, therefore, expect the MR to approach zero at the lowest temperatures. This is indeed observed for the epitaxial film. On the other hand, the polycrystalline films exhibit MR effect both near $T_c$ and at low $T$. The latter relies more on a static magnetic structure as opposed to a dynamic one responsible for the high-temperature effect near $T_c$.

To better understand the source of MR at low temperatures in the polycrystalline samples, we have carried out detailed magnetization measurements as a function of $T$ and $H$. Figure 4 shows the magnetic hysteresis loops at a temperature of 10 K for the polycrystalline and epitaxial LCMO films. The field is applied along the (100) direction in the plane of the substrate for the epitaxial film. Surprisingly, the magnetization ($M$) at high fields is found to be higher for the polycrystalline films than the epitaxial film. Moreover, $M$ increases with decreasing grain size and reaches a value close to the theoretical limit based on spin-only contributions from all Mn ions ($\sim$660 emu/cc). We believe that this is most likely related to residual strain in the film which increases with increasing grain size in the sample. The hysteresis loops at low fields are magnified and shown as an inset in Fig. 4. The hysteresis loops of the polycrystalline films are broader with higher $H_c$ ($\sim$200 Oe) as would be expected for the average of a random orientation of grains. Note that the $M$ of the epitaxial film saturates for fields above 1000 Oe. This is unlike the polycrystalline samples whose $M$ continues to increase slowly up to the highest measuring field.

The low-temperature MR in the polycrystalline films at low fields can be understood in terms of magnetic domain scattering at the boundary regions.[4,6,8] Since the conduction electrons are almost completely polarized inside a magnetic domain, electrons are easily transferred between pairs of $Mn^{+3}$ and $Mn^{+4}$ ions. However, when these electrons travel across grains, strong spin-dependent scattering at the boundaries will lead to a high zero-field $\rho$. Application of a moderately low field can readily align the domains into a parallel configuration causing the $\rho$ to drop substantially. One impor-

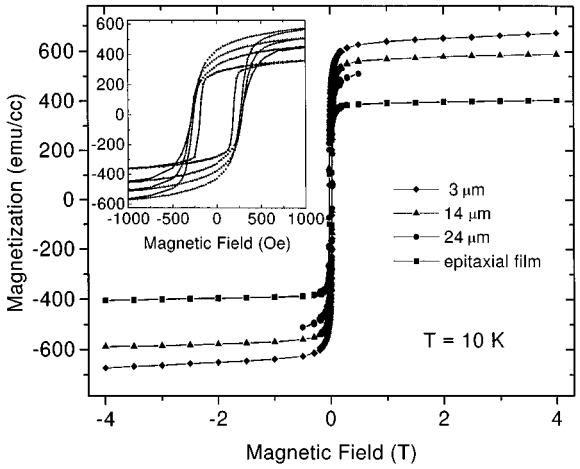


FIG. 4. Magnetic hysteresis loops measured at 10 K for the polycrystalline and epitaxial LCMO thin film samples using a SQUID magnetometer. The low-field loops are shown expanded in the inset.

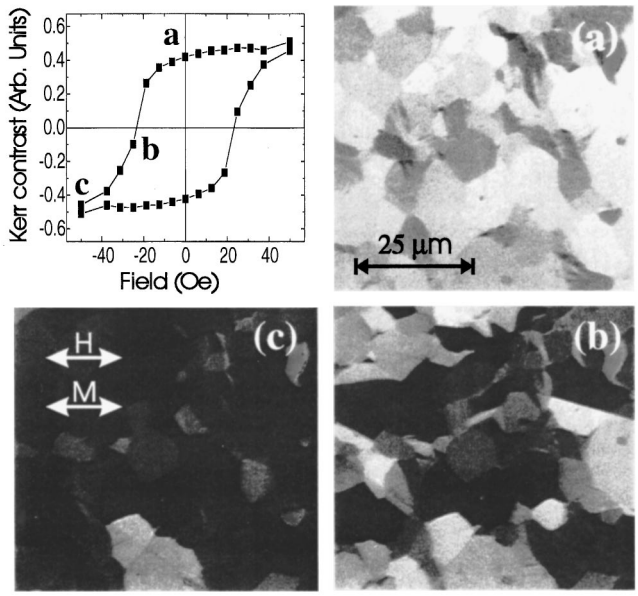


FIG. 5. Kerr hysteresis loop of a polycrystalline LSMO film sample averaged over a number of grains. The three Kerr images correspond to the points (a), (b), and (c) marked in the hysteresis loop. The external field has been applied horizontally, as indicated in the image, and swept between plus and minus 200 Oe. The Kerr signal is sensitive to changes in the horizontal component of the magnetization.

tant conclusion is that it is highly desirable to have an abundance of magnetic domains along the conduction path to enhance the low-field MR.

We have directly imaged the magnetic structure at room temperature in a 1000 Å polycrystalline film of LMSO using a wide-field Kerr microscope.[14] The difficulty of imaging at low temperatures has for the present precluded measurements on LCMO samples. We find that the magnetic domains, which are defined by the grains in the sample, are decoupled and orient successively in a magnetic field. Figure 5 shows a Kerr $M$-$H$ loop of a 14 $\mu$m grain-size polycrystalline film and three corresponding Kerr images. Image (a) displays the nearly uniform magnetic state of the sample at remanence. On moving close to the coercive point, half of the grains switch orientation as seen in image (b). Finally, in image (c) most of the grains have switched as the loop nears saturation. Individual grains can be observed to switch at different fields, and the loop data is an average over the many grains contained in the images. Some of the grains are also observed to switch by wall motion. For example, in the top right corner of (b), a wall can be seen to cross a GB. Wall motion has been observed to be impeded by surface defects such as scratches. Preliminary experiments on epitaxial LSMO films show that, unlike in the polycrystalline samples, magnetization occurs by rotation and domain-wall movement over large areas.

The high-field MR effect in the polycrystalline samples is most likely related to alignment of spins in a magnetically disordered region near the GBs. The spins are canted in this region and are aligned with increasing magnetic field. This is consistent with the fact that the magnetization continues to increase slowly with field in the polycrystalline samples. On application of a large magnetic field, the increasing alignment of the neighboring spins in the canted region leads to a reduction in the resistivity. From extrapolation to high fields, the contribution from the disordered region is estimated to be about 10% of the total magnetization. The decrease in the low-field MR at high temperatures (Fig. 3 inset) may also be partly attributed to the increased scattering in the disordered region.

We finally comment on the relative magnitude of the MR contribution from GB's and the conventional MR observed near $T_c$. It is clear that both magnetic ($\rho_{\mathrm{mag}}$) and structural ($\rho_{\mathrm{str}}$) disorder scattering contribute to the $\rho$ of the polycrystalline films, with different effective lengths existing for the two components. As determined from the slope of the $\rho$ versus $1/L$ plot of the data in Fig. 2, the specific GB $\rho$ at low temperatures decreases with increasing $H$ as the magnetic contribution is reduced. Extrapolating to high fields, we estimate the structural disorder component to be $\sim 2\times 10^{-5}$ $\Omega$ cm$^2$. TEM images indicate that the GB structural disorder thickness is $\sim$10 Å, therefore $\rho_{\mathrm{str}}$ is $\sim$200 $\Omega$ cm. This is about two orders of magnitude higher than the GB $\rho$ of high-$T_c$ oxides.[13] For obtaining $\rho_{\mathrm{mag}}$, it is necessary to have an estimate of the magnetically disordered region. An upper limit is obtained from the Kerr micrographs in Fig. 5. Since no separate contrast is evident near the GB regions in the micrographs, the disorder thickness is estimated to be less than the microscope resolution ($<$5000 Å). This yields a value of $\rho_{\mathrm{mag}} \sim 1$ $\Omega$ cm. Note that as a lower limit, $\rho_{\mathrm{mag}}$ is still about two orders of magnitude higher than $\rho_{\mathrm{max}}$, the peak $\rho$ of the epitaxial film. This suggests that potentially the static MR from the GB region can be significantly larger than the intrinsic MR of the manganites, even at its peak value. From a practical viewpoint, however, the main challenge lies in enhancing the low-field component of the MR by manipulating the formation and movement of magnetic domain boundaries.

We thank T.R. McGuire, Yu Lu, W.J. Gallagher, J. Slonczewski, and P. Chaudhari for useful discussions. This work was partially supported by the NSF under Grant No. DMR-9414160. Y.Y.W. was supported by NSF-STCS, Grant No. DMR 91-20000. V.P.D. was supported by U.S. DOE, Grant No. DE-FG02-92ER45475.

[1] R. von Helmont *et al.*, Phys. Rev. Lett. **71**, 2331 (1993); K. Chahara *et al.*, Appl. Phys. Lett. **63**, 1990 (1993).
[2] S. Jin *et al.*, Science **264**, 413 (1994); S. Manoharan *et al.*, J. Appl. Phys. **76**, 3923 (1994).
[3] H. Y. Hwang *et al.*, Phys. Rev. Lett. **75**, 914 (1995).
[4] H. L. Ju *et al.*, Phys. Rev. B **51**, 6143 (1995).
[5] R. Mahendiran *et al.*, Solid State Commun. **94**, 515 (1995).
[6] A. Gupta *et al.*, Bull. Am. Phys. Soc. **41**, 555 (1996); R. Mahesh *et al.*, Appl. Phys. Lett. **68**, 2291 (1996).
[7] G. Gong *et al.*, Appl. Phys. Lett. **67**, 291 (1995).
[8] P. Schiffer *et al.*, Phys. Rev. Lett. **75**, 3336 (1995).
[9] H. L. Ju *et al.*, Appl. Phys. Lett. **65**, 2108 (1994).
[10] A. Gupta *et al.*, Appl. Phys. Lett. **67**, 3494 (1995).
[11] M. F. Hundley *et al.*, Appl. Phys. Lett. **67**, 860 (1995).
[12] Y. Tokura *et al.*, J. Phys. Soc. Jpn. **63**, 3931 (1994).
[13] For example, see S. E. Babcock and J. L. Vargas, Annu. Rev. Mater. Sci. **25**, 193 (1995).
[14] B. E. Argyle *et al.*, J. Appl. Phys. **61**, 4303 (1987); P. L. Trouilloud *et al.*, IEEE Trans. Magn. **30**, 4494 (1994).
[15] H. Berger, Phys. Status Solidi **1**, 739 (1961).
[16] C. Zener, Phys. Rev. **82**, 403 (1951); P. G. de Gennes, *ibid.* **118**, 141 (1960).